Generating Reactive Virtual Guidance Fixtures for Assisted Telemanipulation Tasks

Santiago Iregui[1,2], Cristian Vergara[1,2], Joris De Schutter[1,2] and Erwin Aertbeliën[1,2]

***Abstract*— In this work, we propose the generation of a tube-shaped virtual fixture that guides the operator towards a target position. This position is obtained through a Human-Machine Interface (HMI) and it is used to adapt the endpoint of the virtual fixture by means of a reactive constraint-based approach. In parallel, a target object is inferred in real-time through a Bayesian intent estimation algorithm that uses information coming from a vision system and the HMI. A shared control strategy is then used to attract the endpoint of the virtual fixture towards the inferred target object. The path of this reactive virtual fixture also adapts to avoid collisions with dynamic obstacles. With our approach, we expect to reduce the effort and fatigue of the operators when performing telemanipulation tasks.**

I. Introduction

According to the world health organization, between 250,000 and 500,000 people become spinal cord injured each year. In order to improve their quality of life, robotic solutions can be used to aid them in performing daily tasks. These solutions should not be fully autonomous, since people with nervous system lesions have the need of recovering autonomy and they want to feel in control as much as possible. Thus, researchers have proposed solutions in which patients can teleoperate robot arms while being assisted by a computer to perform the task (e.g. [1]).

For this reason, we are working on the development of assistive strategies for patients with different levels of mobility. For patients that have very low mobility, a novel invasive visuomotor Brain-Machine Interface (BMI[3]) is planned to be used. Likewise, for patients with higher mobility, other less invasive HMIs, with suitable number of degrees of freedom (DoF), are being explored. Nevertheless, the same control strategies are easily modifiable to match the different HMIs due to our constraint-based approach.

For assisting the operators during telemanipulation tasks, researchers often use virtual fixtures to constrain the desired movement of the robot. In order to deal with the potential change of the target related to the task, Weber et al. [2] present a method where a modeled virtual fixture with immutable shape follows the target. For a similar purpose, we propose the generation of a tube-shaped Reactive Virtual Guidance Fixture (RVGF) that adapt its shape at two levels:

(i) *globally,* to adapt the target position of the RVGF towards goals determined by online intent estimation, while preserving the geometric shape learned from demonstrations;

(ii) *locally,* to perform collision avoidance of dynamic obstacles by deforming locally (i.e. a section of the RVGF), while overcoming the limitations of the learned information.

II. Methodology

Our assistive strategy is implemented within the constraint-based task specification framework eTaSL/eTC [3]. This strategy provides robotic assistance by means of the generation of an RVGF that combines two different behaviors: *(i)* an impedance outside a tube-shaped volume attracts the end effector of the robot towards its interior (where it can move freely), resulting in effective guidance for the operator towards the goal; and *(ii)* an attraction of the end position of the tube allows the proper guidance towards intent-inferred targets.

Behavior (*i*) is obtained by generating the parametrized path $\boldsymbol{f}_{\mathrm{g}}(\boldsymbol{\chi}, s)$ of the tube using (1), where $\bar{\boldsymbol{b}}(s)$ represents the mean of a set of demonstrations. The shape of this path is encoded within the basis functions $\boldsymbol{f}_i(s)$, which are obtained by applying Probabilistic Principal Component Analysis (PPCA) to a small set of demonstrations obtained through kinesthetic teaching. These basis functions, depending on a normalized progress variable s (from 0 to 1), are then modulated by eTaSL feature variables χ_i [4]. This allows us to adapt the RVGF towards new targets while preserving the learned shape.

$$\boldsymbol{f}_{\mathrm{g}}(\boldsymbol{\chi}, s) = \sum_{i=1}^{n} \chi_i \boldsymbol{f}_i(s) + \bar{\boldsymbol{b}}(s). \tag{1}$$

Collisions between the RVGF volume and the obstacles are avoided by placing protective spheres along the RVGF for different values of s (see Fig. 3). This allows the RVGF to react and guide the operator through a collision-free volume. In addition, a set of protective spheres is placed in the gripper to ensure that there is no collision when the operator moves the tool close to the boundaries of the RVGF.

In order to deviate from the obstacle, a set of local basis functions is placed along $\boldsymbol{f}_{\mathrm{g}}$ to allow local deformations of the RVGF. The amplitudes of these basis functions are constrained to be zero, so that the generated RVGF preferably has the same shape of $\boldsymbol{f}_{\mathrm{g}}$. However, in presence of obstacles,

All authors gratefully acknowledge the financial support of KU Leuven C1 project "Neurophysiological investigations of the human and nonhuman primate brain: from perception to action" (3M180301) and of Flanders Make through project SmartHandler_ICON. *(Corresponding author: Santiago Iregui,* santiago.iregui@kuleuven.be)

[1] Robotics Research Group, KU Leuven. [2] Core Lab ROB, Flanders Make@KU Leuven

[3]Research on decoding information such as location, grasping intention, and other useful data through a novel visuomotor BMI, is currently being performed by our project partners in UZ Leuven and imec.

the amplitudes (modeled as feature variables) vary, since the weights of the collision avoidance constraints are higher. This results in a similar spring-like behavior as the one described in [5] when interacting with the obstacle.

Behavior (*ii*) is obtained by means of a shared control between the operator and the computer. The operator control input is given by the decoded target position $\boldsymbol{x}_{\text{hmi}}$ from an HMI. On the other hand, the computer control is given by a Bayesian intent estimation algorithm that infers the desired target object (selected from a set of objects detected by a vision system).

This leads to two conflicting constraints $\boldsymbol{e}_{\text{op}} = \boldsymbol{f}_{\text{g}}(\boldsymbol{\chi}, 1) - \boldsymbol{x}_{\text{hmi}} \rightarrow \boldsymbol{0}$ and $\boldsymbol{e}_{\text{pred}} = \boldsymbol{f}_{\text{g}}(\chi, 1) - \boldsymbol{x}_{\text{pred}} \rightarrow \boldsymbol{0}$, that constrain the endpoint of $\boldsymbol{f}_{\text{g}}$ respectively to $\boldsymbol{x}_{\text{hmi}}$ and the position of the predicted target $\boldsymbol{x}_{\text{pred}}$. The associated weights of these constraints are modulated according to the posterior probability $P(O_{\text{pred}}|\boldsymbol{x}_{\text{hmi}})$ (see Fig. 1a) and determine who is in control (see Fig. 1b). This modulation creates a behavior that attracts the endpoint of the RVGF towards the inferred target object O_{pred} when $P(O_{\text{pred}}|\boldsymbol{x}_{\text{hmi}})$ is above a threshold.

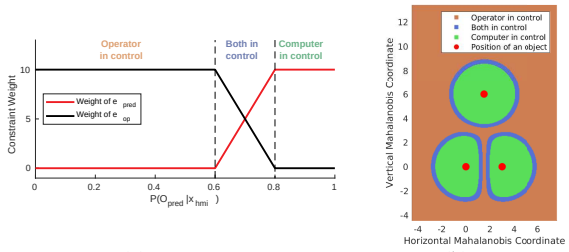

(a) (b)

Fig. 1. Shared control that attracts the end position of the RVGF towards the inferred target object. (a) Constraint weights vs probability, (b) Example of autonomy regions for 3 objects in a 2D dimensionless space (based on the Mahalanobis distance).

III. Results and Discussion

The control strategy was tested in a 7 DoF Kinova Gen3 robot in simulation. An operator with full mobility in the upper limbs commands the target position by using a joystick with the left hand, and controls the position of end effector by using a 3DConnexion SpaceMouse with the right hand[4].

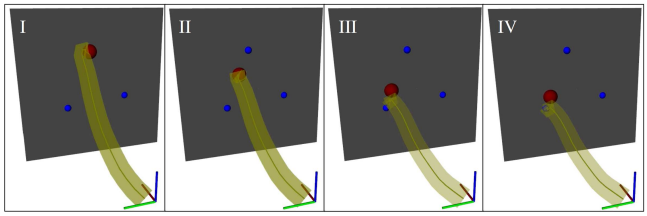

Fig. 2. Snapshots of online change of intention in simulation when the target position is continuously shifted from one target object to another. The red sphere represents the target position, the blue spheres represent known objects, the opaque yellow path represents the center of the RVGF (equal to $\boldsymbol{f}_{\text{g}}(\boldsymbol{\chi}, s)$ when there are no obstacles), and the translucent yellow path represents the tube of the RVGF.

Fig. 2 shows how an RVGF adapts when the goal position $\boldsymbol{x}_{\text{hmi}}$ is continuously shifted from one object to another by a joystick. The goal position coincides with the position of the upper object in snapshot *I* and starts moving towards the bottom left object. Snapshot *II* shows how the RVGF adapts towards $\boldsymbol{x}_{\text{hmi}}$ since $P(O_{\text{pred}}|\boldsymbol{x}_{\text{hmi}})$ is low (left section of Fig.1a). In snapshot *III* the middle section depicted in Fig.1a is reached and the autonomy of the operator and the computer is weighted. Finally, in snapshot *IV* $\boldsymbol{x}_{\text{hmi}}$ is close enough to the object and the end position of the RVGF becomes the position of the object. The parametrized path (1) was generated with PPCA from five demonstrations.

Fig. 3 shows how the robot and the RVGF behave when a dynamic obstacle approaches, while the operator controls the position of the end effector with the SpaceMouse. The RVGF pulls the end effector towards the inner part of the tube-shaped collision-free volume with a specified impedance. Observe in snapshots *II* and *III* how the RVGF adapts its shape due to the collision constraints with the protective spheres. Afterwards, in snapshot *IV* it can be observed how the RVGF recovers its original shape (given by the path $\boldsymbol{f}_{\text{g}}$).

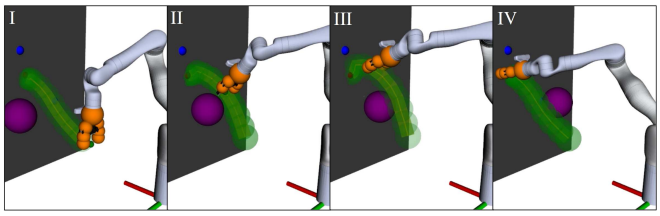

Fig. 3. Snapshots of dynamic obstacle avoidance in simulation. The protective spheres placed along the RVGF and the gripper are depicted in green and in orange, respectively, and the moving obstacle is represented by the purple sphere.

The orientation $\boldsymbol{R}_{\text{tcp}}(s_a)$ of the end effector (see Fig. 3) is autonomously controlled from an initial to a final orientation (the latter will be provided by a vision system). Notice that $\boldsymbol{R}_{\text{tcp}}(s_a)$ is a function of the actual progress variable s_a, which indicates the progress of the end effector along the path $\boldsymbol{f}_{\text{g}}(\boldsymbol{\chi}, s)$.

Operators are expected to be able to control the robot without any significant effort or previous training. In a later phase we plan to perform clinical trials in a physical setup for validation.

[4]This input mode is for demonstration purposes only.

References

[1] K. Muelling, A. Venkatraman, J. S. Valois, J. E. Downey, J. Weiss, S. Javdani, M. Hebert, A. B. Schwartz, J. L. Collinger, and J. A. Bagnell, "Autonomy infused teleoperation with application to brain computer interface controlled manipulation," *Autonomous Robots*, vol. 41, no. 6, pp. 1401–1422, August 2017.

[2] T. Weber Martins, A. Pereira, T. Hulin, O. Ruf, S. Kugler, A. M. Giordano, R. Balachandran, F. Benedikt, J. Lewis, R. Anderl, K. Schilling, and A. Albu-Schäffer, "Space factory 4.0 - new processes for the robotic assembly of modular satellites on an in-orbit platform based on industrie 4.0 approach," in *International Astronautical Congress*, October 2018.

[3] E. Aertbeliën and J. De Schutter, "ETaSL/eTC: A constraint-based task specification language and robot controller using expression graphs," in *IEEE Int. Conf. on Intel. Robots and Systems*, 2014, pp. 1540–1546.

[4] C. A. Vergara, J. De Schutter, and E. Aertbeliën, "Combining imitation learning with constraint-based task specification and control," *IEEE Robot. and Autom. Letters*, vol. 4, no. 2, pp. 1892–1899, April 2019.

[5] O. Brock and O. Khatib, "Elastic strips: A framework for motion generation in human environments," *The International Journal of Robotics Research*, vol. 21, no. 12, pp. 1031–1052, 2002.